



# Efficient CO<sub>2</sub>-Reducing Activity of NAD-Dependent Formate Dehydrogenase from *Thiobacillus* sp. KNK65MA for Formate Production from CO<sub>2</sub> Gas

Hyunjun Choe<sup>1</sup>✉, Jeong Chan Joo<sup>1</sup>✉, Dae Haeng Cho<sup>1</sup>, Min Hoo Kim<sup>2</sup>, Sang Hyun Lee<sup>2</sup>, Kwang Deog Jung<sup>3</sup>, Yong Hwan Kim<sup>1\*</sup>

**1** Department of Chemical Engineering, Kwangwoon University, Seoul, Republic of Korea, **2** Department of Microbial Engineering, Konkuk University, Seoul, Republic of Korea, **3** Clean Energy Research Center, Korea Institute of Science and Technology, Seoul, Republic of Korea

## Abstract

NAD-dependent formate dehydrogenase (FDH) from *Candida boidinii* (CbFDH) has been widely used in various CO<sub>2</sub>-reduction systems but its practical applications are often impeded due to low CO<sub>2</sub>-reducing activity. In this study, we demonstrated superior CO<sub>2</sub>-reducing properties of FDH from *Thiobacillus* sp. KNK65MA (TsFDH) for production of formate from CO<sub>2</sub> gas. To discover more efficient CO<sub>2</sub>-reducing FDHs than a reference enzyme, i.e. CbFDH, five FDHs were selected with biochemical properties and then, their CO<sub>2</sub>-reducing activities were evaluated. All FDHs including CbFDH showed better CO<sub>2</sub>-reducing activities at acidic pHs than at neutral pHs and four FDHs were more active than CbFDH in the CO<sub>2</sub> reduction reaction. In particular, the FDH from *Thiobacillus* sp. KNK65MA (TsFDH) exhibited the highest CO<sub>2</sub>-reducing activity and had a dramatic preference for the reduction reaction, i.e., a 84.2-fold higher ratio of CO<sub>2</sub> reduction to formate oxidation in catalytic efficiency ( $k_{cat}/K_B$ ) compared to CbFDH. Formate was produced from CO<sub>2</sub> gas using TsFDH and CbFDH, and TsFDH showed a 5.8-fold higher formate production rate than CbFDH. A sequence and structural comparison showed that FDHs with relatively high CO<sub>2</sub>-reducing activities had elongated N- and C-terminal loops. The experimental results demonstrate that TsFDH can be an alternative to CbFDH as a biocatalyst in CO<sub>2</sub> reduction systems.

**Citation:** Choe H, Joo JC, Cho DH, Kim MH, Lee SH, et al. (2014) Efficient CO<sub>2</sub>-Reducing Activity of NAD-Dependent Formate Dehydrogenase from *Thiobacillus* sp. KNK65MA for Formate Production from CO<sub>2</sub> Gas. PLoS ONE 9(7): e103111. doi:10.1371/journal.pone.0103111

**Editor:** Joel H. Weiner, University of Alberta, Canada

**Received:** February 28, 2014; **Accepted:** June 27, 2014; **Published:** July 25, 2014

**Copyright:** © 2014 Choe et al. This is an open-access article distributed under the terms of the Creative Commons Attribution License, which permits unrestricted use, distribution, and reproduction in any medium, provided the original author and source are credited.

**Funding:** This work was supported and funded by the Korea CCS R&D Center (KCRC) grant (2013M1A8A1038187), the Converging Research Center Program (2011K000660), the National Research Foundation of Korea (NRF20110029249), and KETEP Grant (20133030000300). The funders had no role in study design, data collection and analysis, decision to publish, or preparation of the manuscript.

**Competing Interests:** The authors have declared that no competing interests exist.

\* Email: metalkim@kw.ac.kr

✉ These authors contributed equally to this work.

✉ Current address: Department of Chemical Engineering and Applied Chemistry, University of Toronto, Toronto, Canada

## Introduction

Reducing the atmospheric CO<sub>2</sub> level has received a great deal of attention recently as an approach to combat global warming and fossil-fuel shortages, but this process remains challenging. Biological CO<sub>2</sub> fixation is one of the most important approaches to solving these problems. Enzymatic CO<sub>2</sub> reduction has been examined extensively as a promising approach to greenhouse gas fixation and the production of renewable fuels and chemicals [1–3]. The enzymatic reduction of CO<sub>2</sub> using FDHs has been widely studied for the production of valuable chemicals, such as formic acid and methanol [4,5]. Formic acid is considered to be a promising replacement for methanol in miniature fuel cells [6]. Formic acid has been produced by the hydrolysis of methyl formate, which is synthesized via methanol carbonylation in commercial processes. Therefore, it would be environmentally attractive to prepare formic acid from CO<sub>2</sub> gas by enzymatic biotransformation.

Many efforts have been made to develop CO<sub>2</sub>-reducing chemical catalysts, and recent research on chemical catalysts has led to improved rates for CO<sub>2</sub> reduction [7,8]. However, chemical

catalysts require harsh reaction conditions and/or expensive metals, such as ruthenium, rhodium, and iridium [9–11]. In contrast to a chemical CO<sub>2</sub> reduction, CO<sub>2</sub> can be reduced by enzymes under mild conditions. There are few biocatalysts capable of biological CO<sub>2</sub> fixation, e.g. pyruvate decarboxylase (EC 4.1.1.1), carbonic anhydrase (EC 4.2.1.1), and FDH (EC 1.2.1.2). Pyruvate decarboxylase can catalyze the reversible conversion of pyruvate into CO<sub>2</sub> and acetaldehyde and thus requires equimolar acetaldehyde for the conversion of CO<sub>2</sub> into pyruvate [3]. It should be noted that carbonic anhydrase can catalyze the rapid interconversion of CO<sub>2</sub> and bicarbonate but this is not a real CO<sub>2</sub> reduction reaction but a CO<sub>2</sub> hydration reaction [12,13]. However, FDH can reduce CO<sub>2</sub> to formate without any other organic chemicals, and formate can be sequentially reduced to formaldehyde and methanol by coupling aldehyde dehydrogenase and alcohol dehydrogenase reactions [4]. Therefore, FDH has been widely adopted in CO<sub>2</sub> reduction reactions [4,14–16]. FDH can be divided into two groups, NAD-independent or NAD-dependent. NAD-independent FDHs have a high CO<sub>2</sub>-reducing activity but include extremely oxygen-labile catalytic components, such as metal ions (tungsten or molybdenum), iron-sulfur clusters,

and selenocysteine, making these FDHs unsuitable for industrial applications [17–20]. Recently, NAD-dependent FDHs have been utilized in CO<sub>2</sub> reduction systems as an alternative to NAD-independent FDHs. In particular, CbFDH is commercially available and has been widely adopted as a CO<sub>2</sub>-reducing biocatalyst in electrochemical, photochemical, and enzymatic reactions [4,14,16] as well as a NADH-regenerating biocatalyst in enzyme-coupled reaction systems [21–24]. However, the CO<sub>2</sub>-reducing activity of CbFDH is still very low for practical applications, and thus it is necessary to discover more efficient FDHs than CbFDH.

In this study, we report superior CO<sub>2</sub>-reducing performance of TsFDH. We selected five FDHs based on their biochemical properties, e.g. acidic optimum pH, specific activity, and stability, and investigated their feasibility as CO<sub>2</sub>-reducing biocatalysts. Enzyme activities in formate oxidation and CO<sub>2</sub> reduction were measured, and the ternary complex model was applied to understand the characteristics of FDHs. Finally, the concentration of formate produced from CO<sub>2</sub> gas using TsFDH and CbFDH was compared. Based on these experimental results, TsFDH can be a good substitute for CbFDH as an efficient CO<sub>2</sub>-reducing biocatalyst.

## Materials and Methods

### Materials

The *fdh* genes used in this study were synthesized with an additional C-terminal hexa-histidine sequence by GenScript (USA). Restriction enzymes were purchased from Takara (Japan). *Pfu* DNA polymerase and ligase were purchased from New England Biolabs (USA). The pET-23b(+) vector and competent cell *E. coli* DH5 $\alpha$ /BL21 ( $\lambda$ DE3) were purchased from Novagen (USA). Ni-NTA resin was purchased from Qiagen (USA). SYPRO Orange dye was purchased from Invitrogen (USA). CbFDH and all chemicals used in enzyme reactions were purchased from Sigma-Aldrich (USA).

**Cloning, expression, and purification of FDHs.** The *fdh* genes containing a C-terminal hexa-histidine sequence in the pUC57 vector were PCR-amplified using primers (Table S1). The amplified fragments were digested by *Nhe* I and *Eco*R I and then cloned into a pET-23b(+) vector. The sequence of recombinant plasmids was confirmed by DNA sequencing (Cosmogenetech, Korea). The recombinant plasmids were chemically transformed into competent *E. coli* BL21 ( $\lambda$ DE3). Expression and purification of the FDHs were performed as previously described [25]. Ni-NTA resin was used to purify the FDHs with a C-terminal hexa-histidine tag. To obtain pure enzymes, the recombinant FDHs were washed with 50 ml of wash buffer (50 mM NaH<sub>2</sub>PO<sub>4</sub> pH 7.0, 300 mM NaCl, 40 mM imidazole), and the purity of the FDHs was determined by 12% SDS-PAGE.

**Determination of conformational stability.** The conformational stability of the FDHs was determined by differential scanning fluorimetry (DSF) using a real-time quantitative PCR thermal cycler (LightCycler 480, Roche, USA). The DSF method can measure the temperatures at the midpoint of a protein's melting transition ( $T_m$ ) by monitoring their thermal unfolding. SYPRO Orange (20x) and 10 to 30  $\mu$ M of purified FDHs were used in 96-well qPCR microplates. The  $T_m$  values were determined by heating from 20 to 95°C at a 1°C/min scan rate as previously described [26].

**Activity assay of FDHs.** The FDH activity was determined by monitoring the absorbance changes at 340 nm during the redox reactions catalyzed by the FDHs at 25°C and different pH values (5.5–7.0). One unit of oxidation activity was defined as the

amount of enzyme required to produce 1  $\mu$ mol of NADH per minute under standard conditions. The oxidation of formate was conducted using an assay solution (2 ml of a 100 mM sodium phosphate buffer) containing 20  $\mu$ g of FDH, 200 mM sodium formate, and 2 mM NAD<sup>+</sup>. One unit of reduction activity was defined as the amount of enzyme required to consume 1  $\mu$ mol of NADH per minute under standard conditions. The reduction of CO<sub>2</sub> was conducted using an assay solution (2 ml of a 100 mM sodium phosphate buffer) containing 3.0 mg of FDH, 50 mM NaHCO<sub>3</sub>, and 0.15 mM NADH. In the case of the CO<sub>2</sub> reduction reaction, NaHCO<sub>3</sub> was used as a substrate to supply CO<sub>2</sub> because the concentration of gaseous CO<sub>2</sub> cannot be accurately determined. Therefore, the substrate concentration for CO<sub>2</sub> reduction was represented as that of NaHCO<sub>3</sub>. A relatively large amount of enzyme was used for CO<sub>2</sub> reduction due to the very low CO<sub>2</sub>-reducing activity of CsFDH. All activities were calculated by subtracting the decomposition rate of NADH in the absence of the enzyme.

**Determination of kinetic parameters.** The saturation concentration of NADH required for CO<sub>2</sub> reduction was too high to adopt the steady-state model and thus the ternary complex model [27] was applied with low concentrations of substrate and cofactors. The kinetic parameters were determined according to the sequential mechanism model proposed by Cleland [28]. This mechanism was described as follows (1):

$$v = \frac{V_{\max}[A][B]}{K_{iA}K_B + K_B[A] + K_A[B] + [A][B]} \quad (1)$$

where  $V_{\max}$  is the maximum reaction rate,  $K_A$  and  $K_B$  are the Michaelis constants for NADH (reduction)/NAD<sup>+</sup> (oxidation) and NaHCO<sub>3</sub> (reduction)/formate (oxidation), respectively, in the presence of saturating concentrations of the other substrate.  $K_{iA}$  is the dissociation constant for the enzyme-cofactor complex. The model was fitted to the experimental data using SigmaPlot (Version 10.0, Systat Software Inc., USA).

The kinetic parameters of the FDH-catalyzed oxidation and reduction reactions were determined in 100 mM sodium phosphate buffer (pH 7.0) with a 1.1 ml reaction volume at 25°C. To perform the formate oxidation reaction, the content of FDHs was fixed at 5  $\mu$ g, while the concentration of NAD<sup>+</sup> varied from 0.1 to 0.3 mM and that of sodium formate varied from 10 to 50 mM. The reduction reaction of CO<sub>2</sub> was achieved with 10 and 100  $\mu$ g of TsFDH and CbFDH, respectively, and the ranges of concentrations for NADH and sodium bicarbonate were same as those of NAD<sup>+</sup> and sodium formate for the formate oxidation reaction. The initial rates of the reactions were determined by measuring the change in NADH.

**Formate production from CO<sub>2</sub> gas.** Sodium phosphate buffer (100 mM, pH 7.0) was purged with CO<sub>2</sub> for 1 h and adjusted to pH 7.0 with NaOH. Formate production reactions were performed by 4.4  $\mu$ M FDHs (1.0 mg of TsFDH or 0.9 mg of CbFDH) with 10 mM NADH. The total volume of reaction solution was 5 ml. The reaction solution was mixed with a magnetic stir bar at 200 rpm and was purged continuously with CO<sub>2</sub> at a flow rate of 50 ml/min during the CO<sub>2</sub> reduction reactions. The amount of formate produced was determined by high-pressure liquid chromatography (HPLC) equipped with an Aminex HPX 87-H ion exclusion column (300 $\times$ 7.8 mm) and a refractive index detector (RID). The temperature of the column and the RID detector was set to 35°C. H<sub>2</sub>SO<sub>4</sub> solution (5 mM) was used as the mobile phase at a flow rate of 0.6 ml/min. Forty microliters of the sample was injected into HPLC for analysis.

## Results

### Production of recombinant NAD-dependent FDHs

The *fdh* genes encoding FDHs from *Ancylobacter aquaticus* KNK607M (AaFDH, BAC65346.1) [29], *Ceriporiopsis subvermispora* (CsFDH, BAF98206.1) [30], *Moraxella* sp. C-1 (MsFDH, CAA73696.1), *Paracoccus* sp. 12-A (PsFDH, BAB64941.1) [31], and *Thiobacillus* sp. KNK 65MA (TsFDH, BAC92737.1) [32] as well as the gene for CbFDH (CAA09466.2) were synthesized, and all recombinant FDHs were successfully expressed with a C-terminal hexa-histidine tag in *E. coli*. The SDS-PAGE gel exhibited the molecular masses of the single subunits that were identical to the calculated molecular mass of AaFDH (45 kDa), CbFDH (41 kDa), CsFDH (40 kDa), MsFDH (45 kDa), PsFDH (45 kDa), and TsFDH (45 kDa) and showed that the recombinant FDHs had a high purity (Fig. 1).

The conformational stability of the FDHs was determined by evaluating their thermal unfolding using the DSF method as previously described [25], and all FDHs were sufficiently stable ( $T_m = 42.3 \sim 61.8^\circ\text{C}$ ) under ambient conditions (Fig. S1).

### Enzyme activities for formate oxidation and CO<sub>2</sub> reduction

The activities of the recombinant FDHs, including CbFDH, in the oxidation and reduction reactions are shown in Fig. 2. All enzyme activities were determined by measuring the initial rates of reaction. All FDHs except for CsFDH had higher enzyme activities in the formate oxidation reaction than CbFDH. CsFDH activity was 1.0~1.3 U/mg enzyme at all tested pH ranges (Fig. 2A). AaFDH exhibited the highest activity, and its enzyme activity was 5.2-fold (20.0 U/mg enzyme) and 3.0-fold (18.3 U/mg enzyme) higher than those of CbFDH at pH 5.5 and 7.0, respectively. The FDHs did not exhibit a drastic change in formate oxidation activity at the tested pH ranges. The CO<sub>2</sub>-reducing activities of FDHs are shown in Fig. 2B. Compared to the formate oxidation activity, all FDHs exhibited low enzyme activities (0.5~12.2 mU/mg) in the CO<sub>2</sub> reduction reaction and had an acidic optimum pH (pH 5.5 or 6.0). Four screened FDHs (AaFDH, MsFDH, PsFDH, and TsFDH) were more active over the pH range of 5.5 to 7.0 than CbFDH, and TsFDH had the

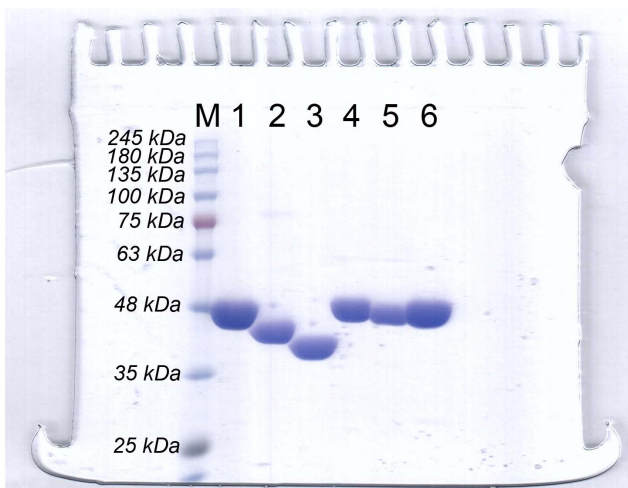


**Figure 1. SDS-PAGE analysis of purified FDHs.** Lane M: molecular mass marker, 1: AaFDH, 2: CbFDH, 3: CsFDH, 4: MsFDH, 5: PsFDH, 6: TsFDH.

doi:10.1371/journal.pone.0103111.g001

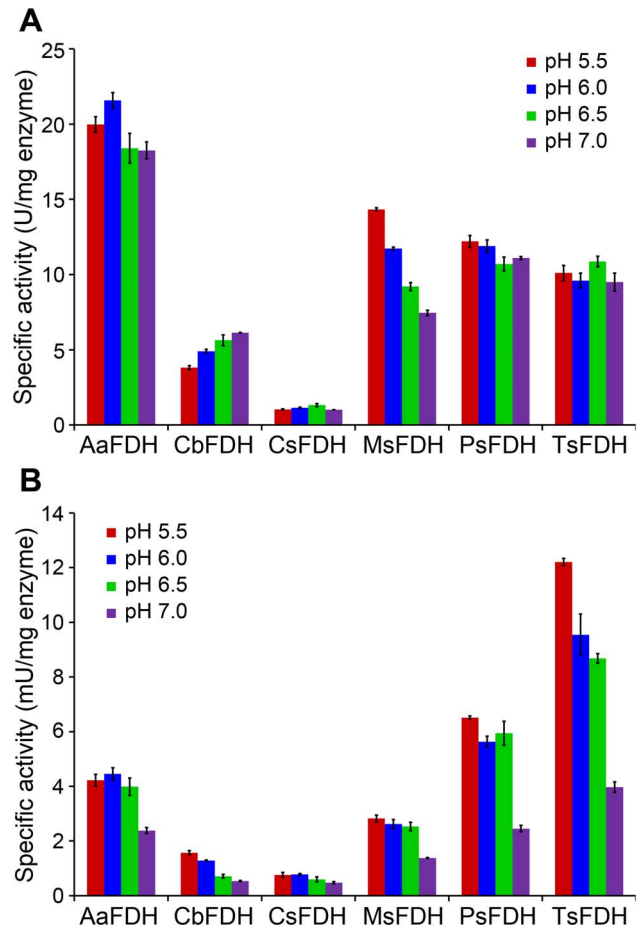


**Figure 2. Enzyme activities of FDHs.** Enzyme activities of FDHs for A) formate oxidation and B) CO<sub>2</sub> reduction at different pH values. doi:10.1371/journal.pone.0103111.g002

highest CO<sub>2</sub>-reducing activity. Its activities were at least 7.3-fold higher (12.2, 9.5, 8.7, and 4.0 mU/mg enzyme) than those of CbFDH (1.6, 1.3, 0.7, and 0.5 mU/mg enzyme) at pH 5.5, 6.0, 6.5, and 7.0, respectively.

### Enzyme kinetics

The kinetic parameters of TsFDH and CbFDH were determined at pH 7.0 because NADH is slowly degraded at acidic pHs [33], resulting in unreliable kinetic values at acidic pHs. Initial rates were measured with respect to cofactors at various fixed concentrations of substrates. Kinetic parameters for the forward and reverse reaction were obtained by fitting the initial rates to equation (1) with non-linear regression (Table 1). Regression coefficients ( $r^2$ ) for all reactions were over 0.937 (Fig. 3). In the formate oxidation reaction, TsFDH showed a lower substrate binding affinity ( $K_B$ , 16.24 mM) and a higher turnover number ( $k_{cat}$ , 1.769/s) than CbFDH (8.55 mM and 1.081/s, respectively), and both enzymes exhibited similar catalytic efficiencies ( $k_{cat}/K_B$ ). In the CO<sub>2</sub> reduction reaction, however, TsFDH had a 3.4-fold higher substrate-binding affinity ( $K_B$ , 9.23 mM), a 21.2-fold higher turnover number ( $k_{cat}$ , 0.318/s), and a 85-fold higher catalytic efficiency ( $k_{cat}/K_B$ , 0.034/mM·s) than CbFDH (31.28 mM, 0.015/s, and 0.0004/mM·s, respectively). TsFDH exhibited a dramatic preference for the reduction reaction with a 84.2-fold higher catalytic efficiency ratio of CO<sub>2</sub> reduction to formate oxidation than that of CbFDH. The recombinant

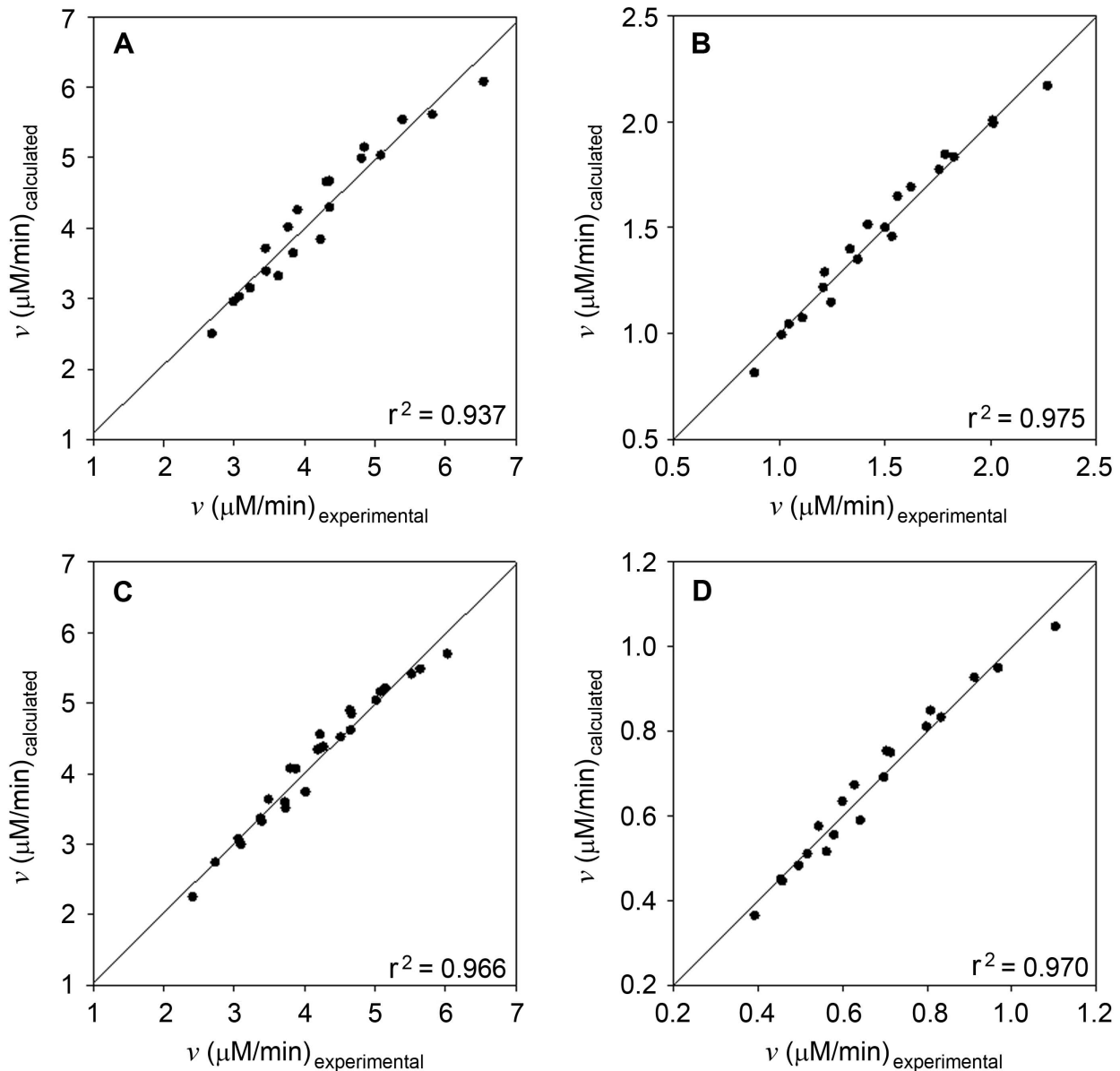


**Figure 3. Determination of kinetic parameters.** Correlation between the measured and calculated initial rates of TsFDH-catalyzed A) formate oxidation and B) CO<sub>2</sub> reduction; CbFDH-catalyzed C) formate oxidation and D) CO<sub>2</sub> reduction.  
doi:10.1371/journal.pone.0103111.g003

CbFDH expressed in *E. coli* and commercial CbsFDH (Sigma-Aldrich) showed similar catalytic efficiencies for the forward and reverse reaction (data not shown) and thus only the data from the recombinant CbFDH was reported in this paper.

#### Formate production through enzymatic CO<sub>2</sub> reduction

Formate was produced from CO<sub>2</sub> gas using TsFDH and CbFDH. The amount of formate produced through the enzymatic CO<sub>2</sub> reduction is shown in Fig. 4. TsFDH and CbFDH produced 0.74 mM and 0.13 mM formate in 120 min, respectively. The formate production rate of TsFDH and CbFDH was linear, with a constant rate of 0.023/s and 0.004/s, respectively. TsFDH showed a 5.8-fold higher formate production rate than CbFDH, which is consistent with the results shown in Fig. 2B.

#### Discussion

FDHs can catalyze the conversion of CO<sub>2</sub> and formate and thus are of great interest as CO<sub>2</sub>-reducing biocatalysts for CO<sub>2</sub> sequestration and for the production of formate as a source of fuels and commodity chemicals. NAD-independent FDHs can drive the CO<sub>2</sub> reduction reaction with electrons supplied from an electrode and artificial electron mediators, such as methyl viologen, exhibiting very high CO<sub>2</sub>-reducing catalytic efficiency [20,34]. Despite this advantage, the use of NAD-independent FDHs in CO<sub>2</sub> reduction systems does not appear to be practical due to the requirement for complicated catalytic components, such as molybdopterin cofactor, iron-sulfur clusters, and selenocysteine, in addition to their oxygen-labile activity, which results in insoluble and inactive expression in *E. coli* [35–37]. Recently, K. Schuchmann and V. Müller reported that a hydrogen-dependent carbon dioxide reductase (HDCR) from

**Table 1.** The kinetic parameters of FDHs<sup>[a]</sup>.

	$K_A$ (mM)	$K_{iA}$ (mM)	$K_B$ (mM)	$k_{cat}$ (1/s)	$k_{cat}/K_B$ (1/mM·s)	$\frac{(k_{cat}/K_B)_{reverse}}{(k_{cat}/K_B)_{forward}}$
TsFDH <sup>[b]</sup>	0.281±0.081	0.005±0.002	16.24±5.39	1.769±0.441	0.109	3.2×10 <sup>-1</sup>
TsFDH <sup>[c]</sup>	0.264±0.076	0.126±0.053	9.23±3.98	0.318±0.051	0.034	
CbFDH <sup>[b]</sup>	0.102±0.030	0.134±0.087	8.55±2.56	1.081±0.109	0.126	3.8×10 <sup>-3</sup>
CbFDH <sup>[c]</sup>	0.512±0.186	0.014±0.010	31.28±8.05	0.015±0.005	0.0004	

<sup>[a]</sup>Kinetic parameters for the forward (formate oxidation) and reverse (CO<sub>2</sub> reduction) reactions were calculated by fitting the initial rates to equation (1).

<sup>[b]</sup>Formate oxidation (A: NAD<sup>+</sup>, B: sodium formate).

<sup>[c]</sup>CO<sub>2</sub> reduction (A: NADH, B: sodium bicarbonate).

doi:10.1371/journal.pone.0103111.t001

*Acetobacterium woodii* can catalyze reduction of CO<sub>2</sub> to formate with very high activity [38]. However, it is also very unstable under aerobic conditions as it has the catalytic components (Table S2). In contrast to NAD-independent FDHs and HDCR, NAD-dependent FDHs are oxygen-stable and can be highly expressed in *E. coli* as demonstrated in this study, but their practical applications in CO<sub>2</sub>-reduction systems are still limited due to their low CO<sub>2</sub>-reducing activities.

In this study, we attempted to identify FDHs that are superior to a conventional CO<sub>2</sub>-reducing biocatalyst, i.e., CbFDH. FDHs suitable for CO<sub>2</sub> reduction were screened from BRENDA (BRaunschweig ENzyme Database, <http://www.brenda-enzymes.org>) [39] based on their optimum pH. The catalytic mechanism of formate oxidation by NAD-dependent FDHs has been demonstrated to involve direct hydride transfer from formate to the C4 atom of the nicotine amide ring of NAD<sup>+</sup> [40,41]. However, it remains unclear whether NAD-dependent FDHs use a proton-relay system in the CO<sub>2</sub> reduction reaction. The abundance of protons would be favorable for the reduction of many chemicals [42,43]. Moreover, Peacock and Boulter reported that FDH from *Phaseolus aureus* (PaFDH) had 19.7-fold higher CO<sub>2</sub>-reducing activity at pH 6.3 than at pH 8.0 (710 pmol/min vs. 36 pmol/min) with approximately equivalent concentrations of enzyme and substrate and showed a 19.6-fold lower ratio of the rates of the forward (formate oxidation) and reverse (CO<sub>2</sub> reduction) reaction (2,300 at pH 6.3 vs. 45,000 at pH 8.0) [27]. These results imply that FDHs with an acidic optimum pH would

be more efficient for CO<sub>2</sub> reduction than FDHs with neutral or alkaline optimum pH. In the present study, the preliminary experiment also revealed that CbFDH has a higher CO<sub>2</sub>-reducing activity at an acidic pH (1.6 mU/mg enzyme at pH 5.5) than at a neutral pH (0.5 mU/mg enzyme at pH 7.0), whereas it exhibited higher formate-oxidation activity at a neutral pH (6.1 U/mg enzyme at pH 7.0) than at an acidic pH (3.8 U/mg enzyme at pH 5.5) (Fig. 2). In addition, it has been reported that CO<sub>2</sub>, bicarbonate (HCO<sub>3</sub><sup>-</sup>), and carbonate (CO<sub>3</sub><sup>2-</sup>) are dominant at acidic, neutral, and alkaline pHs, respectively [44]. As mentioned above, CO<sub>2</sub> reduction at an acidic pH has apparent advantages over reduction under neutral or alkaline pH conditions, including the presence of abundant protons, a high CO<sub>2</sub> fraction [42], and higher CO<sub>2</sub>-reducing activity of FDHs. Therefore, we selected five NAD-dependent FDHs (AaFDH, CsFDH, MsFDH, PsFDH, and TsFDH) with an acidic optimum pH and comparable activity and stability to those of the reference enzyme CbFDH. All FDHs were successfully expressed and purified with Ni-NTA resin (Fig. 1). The five FDHs characterized in this study showed an acidic optimum pH for formate oxidation and CO<sub>2</sub> reduction and moderate stability under ambient conditions (Table S3).

As shown in Fig. 2, AaFDH had the highest enzyme activity in the oxidation reaction, which was at least 3-fold higher than that of CbFDH. High formate oxidation activity and the DSF results (Table S3) indicate that AaFDH could be used as an alternative NADH-regenerating enzyme to CbFDH over a broad pH range. In the reduction reaction, all enzymes, including CbFDH, exhibited an acidic pH optimum, indicating that an acidic pH is more favorable than neutral pH for CO<sub>2</sub> reduction. The lowest values for the ratio of the rates of the oxidation and reduction reaction were calculated as 4,600 at pH 6.5, 2,400 at pH 5.5, 1,400 at pH 5.5, 3,600 at pH 6.5, 1,800 at pH 6.5, and 820 at pH 5.5 for AaFDH, CbFDH, CsFDH, MsFDH, PsFDH, and TsFDH (obtained from Fig. 2), which are comparable to the value of PaFDH [27]. All FDHs showed better reduction activities at acidic pH than at neutral pH. TsFDH was the best biocatalyst in terms of CO<sub>2</sub>-reducing activity and the ratio of the rates of the oxidation and reduction reactions.

Previous enzyme kinetics revealed that FDHs have a sequential mechanism in which both substrates bind to the enzyme in a defined or random order before the products are released. Eukaryotic FDHs catalyze formate oxidation by an ordered kinetic mechanism, but bacterial FDHs follow a random mechanism with a rapid equilibrium [27,40]. The Michaelis-Menten plots were obtained (Fig. S2). Saturation of NaHCO<sub>3</sub> and NADH is very difficult for the CO<sub>2</sub> reduction reaction. Saturation of NADH for enzyme-catalyzed CO<sub>2</sub> reduction could not be achieved by high degradation rate of NADH and inhibitory effect

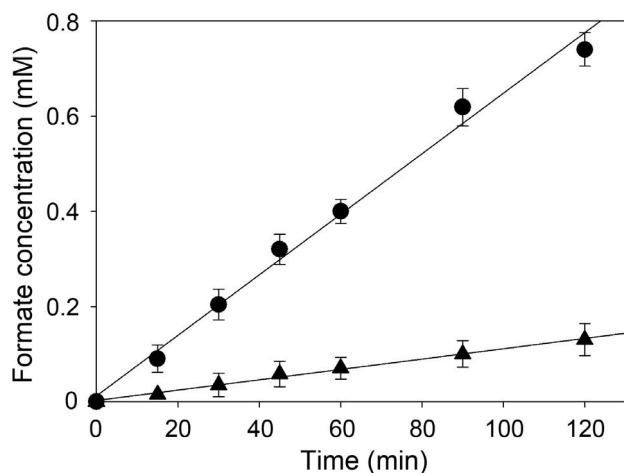


**Figure 4. Formate production through FDH-catalyzed CO<sub>2</sub> reduction.** Formate production by (●) TsFDH and (▲) CbFDH in 100 mM sodium phosphate buffer, pH 7.0. doi:10.1371/journal.pone.0103111.g004

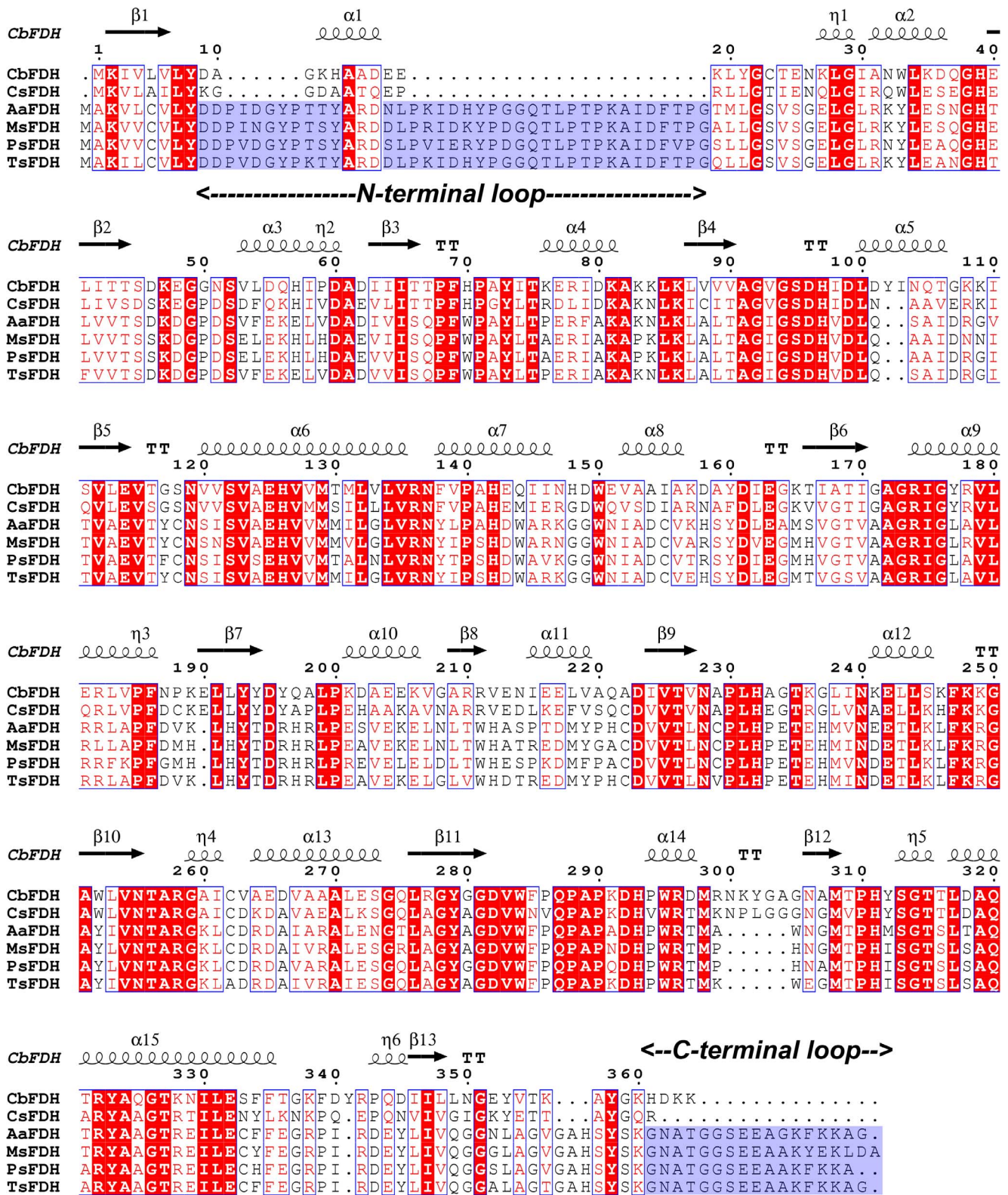
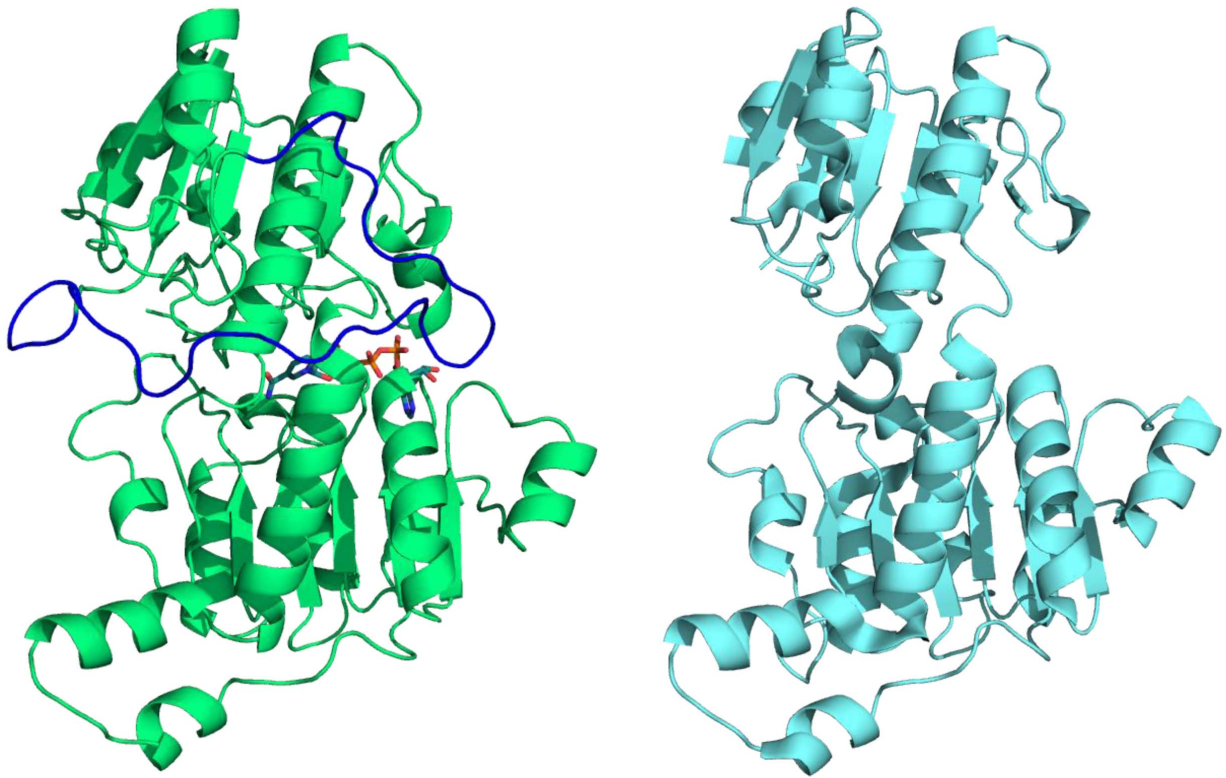


**Figure 5. Sequence alignment of NAD-dependent FDHs.** Amino acid sequences of FDH from yeast: CbFDH; FDH from fungi: CsFDH; FDHs from bacteria: AaFDH, MsFDH, PsFDH, and TsFDH. The blue background indicates the additional sequence regions for the N- and C-terminal loops of bacterial FDHs. Conservative amino acids are represented in red box and secondary structure elements are assigned according to the structure of CbFDH (pdb code: 2FSS).

doi:10.1371/journal.pone.0103111.g005

A



B

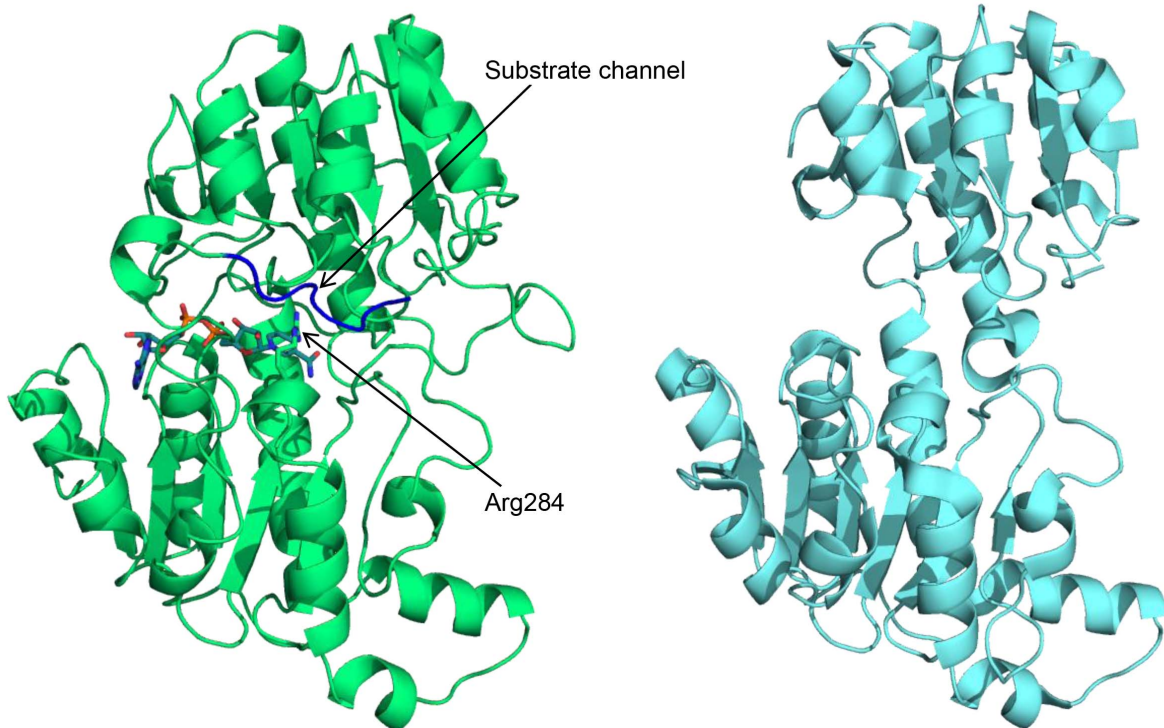


**Figure 6. Structural comparison of TsFDH and CbFDH.** Structural comparison of the A) N- and B) C-terminal loops of TsFDH (green, modeled using 2NAD) and CbFDH (cyan, pdb code: 2F5S). The elongated N- and C-terminal loops are shown in blue.  
doi:10.1371/journal.pone.0103111.g006

of degraded compounds. The reaction rate was decreased with increasing NADH concentration of over 0.4 mM [45]. Low solubility of CO<sub>2</sub> in buffer at atmospheric pressure also caused the difficulty of CO<sub>2</sub> saturation for enzyme-catalyzed CO<sub>2</sub> reduction. Therefore, typical Michaelis-Menten saturation plot which shows the convergence of velocity to  $v_{\max}$  could not be obtained. However, kinetic constants could be obtained on the basis of generally acceptable rapid equilibrium assumption for enzyme-substrate complex. Double reciprocal plots of eukaryotic CbFDH and bacterial TsFDH were linear and gave intersecting patterns in the forward and reverse reaction (Fig. S3), indicating that the kinetic mechanism of both FDHs is sequential. Both FDHs exhibited a similar binding affinity for formate, which is comparable to that of typical NAD-dependent FDHs (1~15 mM) [40]. Both FDHs had a similar catalytic efficiency ( $k_{\text{cat}}/K_{\text{B}}$ ) in the oxidation of formate, but TsFDH showed a dramatic preference for CO<sub>2</sub> reduction due to the 21.2-fold higher turnover number compared to CbFDH. These catalytic properties enable TsFDH to produce formate from CO<sub>2</sub> gas more efficiently than CbFDH without the saturation of the reaction rate (Fig. 4). Conventional CO<sub>2</sub> reduction systems using commercial CbFDH for the production of formate or methanol require *in situ* regeneration of NADH to drive CO<sub>2</sub> reduction [4]. The formate production rate of TsFDH can be further improved by incorporating a NADH-regeneration system e.g., chemical, electrochemical, photochemical, or enzymatic method [46]. At an acidic pH, despite high TsFDH-catalyzed CO<sub>2</sub> reduction reaction, it is evident that formate productivity will be gradually decreased due to degradation of NADH under acidic conditions [47]. Recently, various NAD analogs including thio-NAD, APAD, PAAD, and NAAD were found to be more efficient and stable than NAD in electrochemical regeneration systems [48]. Thus, these analogs need to be investigated as an alternative cofactor to overcome the instability NADH at an acidic pH.

Tishkov and Popov performed structural and multiple sequence alignment of eukaryotic FDHs and bacterial FDHs and found that bacterial FDHs have an addition loop in the N-terminal end, which may have an important role in the discrimination of the kinetic mechanism of the two different groups of FDHs [40]. In this study, it should be noted that four bacterial FDHs showed higher CO<sub>2</sub>-reducing activities than two eukaryotic FDHs. Multiple sequence alignment of six FDHs was conducted using CLUSTAW2 and ESPrpt 2.2 [49,50] (Fig. 5). The FDHs tested in this study can be classified into two groups (bacterial FDHs, AaFDH, MsFDH, PsFDH, and TsFDH, vs. eukaryotic FDHs, yeast CbFDH and fungal CsFDH) as previously described [40]. Bacterial FDHs had at least 82.5% sequence identity, and CbFDH and CsFDH shared 61.2% sequence identity. Although all the amino acids critical for catalysis or cofactor binding are highly conserved [51] in both FDH groups, bacterial FDHs contained an elongated N-terminal loop and C-terminal loop compared to eukaryotic FDHs (Fig. 5). The N-terminal loop may be involved in the determination of the kinetic mechanism, i.e., an ordered or a random model, and the C-terminal loop may contribute to the better CO<sub>2</sub>-reducing activities of bacterial FDHs than those of eukaryotic FDHs. To understand the amino acid differences of FDHs at molecular level, the structural alignment of TsFDH and CbFDH was performed. The structure of TsFDH was modeled using SWISS-MODEL homology modeling [52]. The holo-crystal structure of NAD-dependent FDH from *Pseudomonas* sp. 101 (PdFDH, pdb code: 2NAD) was used as a template (92.0% sequence identity with TsFDH) for homology modeling of TsFDH structure because the C-terminal loop, which covers the substrate channel, is only present in the holo-structure: the loop may be

largely fluctuated in the apo-structure (pdb code: 2NAC). The N-terminal loop covers a significant part of the enzyme (Fig. 6A), and some amino acids in the loop interact with other amino acids of the subunit or the other chain in a dimeric form (structures not shown). However, the N-terminal loop does not have direct interactions with the substrate binding pocket. It was reported that PdFDH has a narrow substrate channel, and Arg284 on the wall of the substrate channel provides conformational mobility for binding and delivery of substrates [53]. In addition, Arg284 has close contacts with an inhibitor i.e. azide in the ternary complex structure (enzyme-NAD-azide, pdb code: 2NAD). Based on this structure information of PdFDH, it can be speculated that upon sequential binding of cofactor and substrate the C-terminal loop can be formed and then, contribute to conformational changes of the substrate channel including Arg284 for enzyme catalysis. The C-terminal loop, which is not present in the structure of CbFDH, in the modeled structure of TsFDH also covers the substrate binding channel, including Arg284 (Fig. 6B). This structural feature of TsFDH may be associated with CO<sub>2</sub> accessibility or binding to the active site given that the kinetics data revealed that TsFDH exhibited a better  $K_{\text{B}}$  value than CbFDH (Table 1). However, we do not yet know whether the loops play important roles in CO<sub>2</sub> binding or catalytic motion in the bacterial FDHs. Although there are many crystal structures and abundant biochemical information on NAD-dependent FDHs, the functions of these loops remains unclear. We plan to prepare a TsFDH C-terminal loop deletion mutant to test the hypothesis.

In summary, five FDHs with acidic optimum pH identified from biochemical data were tested for CO<sub>2</sub> reduction. The superior CO<sub>2</sub>-reducing activity of TsFDH was confirmed by enzyme kinetics and formate production from CO<sub>2</sub> gas. We propose that TsFDH is an alternative to the conventional CO<sub>2</sub>-reducing biocatalyst CbFDH. However, further experiments, including protein engineering and the development of NADH-regeneration systems, will be required to improve the CO<sub>2</sub>-reducing efficiency of TsFDH.

## Supporting Information

**Figure S1 Thermal unfolding curves of the FDHs measured by the DSF method.** AaFDH (blue), CbFDH (red), CsFDH (green), MsFDH(magenta), PsFDH (cyan), and TsFDH (dark gray). (TIF)

**Figure S2 Michaelis-Menten plot for kinetic study.** Michaelis-Menten plots of TsFDH-catalyzed A) formate oxidation and B) CO<sub>2</sub> reduction and CbFDH-catalyzed C) formate oxidation and D) CO<sub>2</sub> reduction. (TIF)

**Figure S3 Lineweaver-Burk plot for kinetic study.** Double reciprocal plots of initial rates of TsFDH-catalyzed A) formate oxidation and B) CO<sub>2</sub> reduction; CbFDH-catalyzed C) formate oxidation and D) CO<sub>2</sub> reduction with various sodium formate and sodium bicarbonate concentrations (●: 10 mM, ▲: 20 mM, ▼: 30 mM, ■: 50 mM). a) and b) in insets show the secondary plots of the slopes and intercepts against the reciprocal concentration of invariant substrate, respectively. (TIF)

**Table S1 The primers used in this study.** (DOCX)

**Table S2 Comparison of the characteristics of TsFDH and other CO<sub>2</sub> reductases.** (DOCX)



**Table S3 Biochemical properties of the FDHs studied in this study.**

(DOCX)

**References**

- Baskaya FS, Zhao X, Flickinger MC, Wang P (2010) Thermodynamic feasibility of enzymatic reduction of carbon dioxide to methanol. *Appl Biochem Biotechnol* 162: 391–398.
- Crabble BR, Plugge CM, McInerney MJ, Stams AJM (2011) Formate formation and formate conversion in biological fuels production. *Enzyme Res* 2011: 532536. doi: 10.4061/2011/532536.
- Tong X, El-Zahab B, Zhao X, Liu Y, Wang P (2011) Enzymatic synthesis of L-lactic acid from carbon dioxide and ethanol with an inherent cofactor regeneration cycle. *Biotechnol Bioeng* 108: 465–469.
- El-Zahab B, Donnelly D, Wang P (2008) Particle-tethered NADH for production of methanol from CO<sub>2</sub> catalyzed by coimmobilized enzymes. *Biotechnol Bioeng* 99: 508–514.
- Lee HJ, Lee SH, Park CB, Won K (2011) Coenzyme analogs: Excellent substitutes (not poor imitations) for electrochemical regeneration. *Chem Commun* 47: 12538–12540.
- Jung WS, Han J, Ha S (2007) Analysis of palladium-based anode electrode using electrochemical impedance spectra in direct formic acid fuel cells. *J Power Sources* 173: 53–59.
- Sakakura T, Choi JC, Yasuda H (2007) Transformation of carbon dioxide. *Chem Rev* 107: 2365–2387.
- North M, Pasquale R, Young C (2010) Synthesis of cyclic carbonates from epoxides and CO<sub>2</sub>. *Green Chem* 12: 1514–1539.
- Federsel C, Ziebart C, Jackstell R, Baumann W, Beller M (2012) Catalytic hydrogenation of carbon dioxide and bicarbonates with a well-defined cobalt dihydrogen complex. *Chem Eur J* 18: 72–75.
- Park S, Bézier D, Brookhart M (2012) An efficient iridium catalyst for reduction of carbon dioxide to methane with trialkylsilanes. *J Am Chem Soc* 134: 11404–11407.
- Sekezawa K, Maeda K, Domen K, Koike K, Ishitani O (2013) Artificial Z-scheme constructed with a supramolecular metal complex and semiconductor for the photocatalytic reduction of CO<sub>2</sub>. *J Am Chem Soc* 135: 4596–4599.
- Kanth BK, Lee J, Pack SP (2013) Carbonic anhydrase: Its biocatalytic mechanisms and functional properties for efficient CO<sub>2</sub> capture process development. *Eng Life Sci* 13: 422–431.
- Jo BH, Kim IG, Seo JH, Kang DG, Cha HJ (2013) Engineered *Escherichia coli* with periplasmic carbonic anhydrase as a biocatalyst for CO<sub>2</sub> sequestration. *Appl Environ Microbiol* 79: 6697–6705.
- Kim S, Lee GY, Lee J, Rajkumar E, Baeg JO, et al. (2013) Efficient electrochemical regeneration of nicotinamide cofactors using a cyclopentadienyl-rhodium complex on functionalized indium tin oxide electrodes. *Electrochim Acta* 96: 141–146.
- Parkinson BA, Weaver PF (1984) Photoelectrochemical pumping of enzymatic CO<sub>2</sub> reduction. *Nature* 309: 148–149.
- Yadav RK, Baeg JO, Oh GH, Park NJ, Kong KJ, et al. (2012) A photocatalyst-enzyme coupled artificial photosynthesis system for solar energy in production of formic acid from CO<sub>2</sub>. *J Am Chem Soc* 134: 11455–11461.
- Almendra MJ, Brondino CD, Gavel O, Pereira AS, Tavares P, et al. (1999) Purification and characterization of a tungsten-containing formate dehydrogenase from *Desulfovibrio gigas*. *Biochemistry* 38: 16366–16372.
- Cone JE, Martin Del Rio R, Davis JN, Stadtman TC (1976) Chemical characterization of the selenoprotein component of clostridial glycine reductase: Identification of selenocysteine as the organoselenium moiety. *Proc Natl Acad Sci U S A* 73: 2659–2663.
- Graentzdoerfer A, Rauh D, Pich A, Andreesen JR (2003) Molecular and biochemical characterization of two tungsten- and selenium-containing formate dehydrogenases from *Eubacterium acidaminophilum* that are associated with components of an iron-only hydrogenase. *Arch Microbiol* 179: 116–130.
- Reda T, Plugge CM, Abram NJ, Hirst J (2008) Reversible interconversion of carbon dioxide and formate by an electroactive enzyme. *Proc Natl Acad Sci U S A* 105: 10654–10658.
- Bommarius AS, Schwarm M, Drauz K (1998) Biocatalysis to amino acid-based chiral pharmaceuticals - Examples and perspectives. *J Mol Catal B: Enzym* 5: 1–11.
- Gröger H, Hummel W, Rollmann C, Chamouleau F, Hüsken H, et al. (2004) Preparative asymmetric reduction of ketones in a biphasic medium with an (S)-alcohol dehydrogenase under *in situ*-cofactor-recycling with a formate dehydrogenase. *Tetrahedron* 60: 633–640.
- Van Der Donk WA, Zhao H (2003) Recent developments in pyridine nucleotide regeneration. *Curr Opin Biotechnol* 14: 421–426.
- Weckbecker A, Hummel W (2004) Improved synthesis of chiral alcohols with *Escherichia coli* cells co-expressing pyridine nucleotide transhydrogenase, NADP<sup>+</sup>-dependent alcohol dehydrogenase and NAD<sup>+</sup>-dependent formate dehydrogenase. *Biotechnol Lett* 26: 1739–1744.
- Kim T, Joo JC, Yoo YJ (2012) Hydrophobic interaction network analysis for thermostabilization of a mesophilic xylanase. *J Biotechnol* 161: 49–59.
- Phillips K, de la Peña AH (2011) The combined use of the ThermoFluor assay and ThermoQ analytical software for the determination of protein stability and buffer optimization as an aid in protein crystallization. *Curr Protoc Mol Biol* Chapter 10: Unit 10.28.
- Peacock D, Boulter D (1970) Kinetic studies of formate dehydrogenase. *Biochem J* 120: 763–769.
- Cleland WW (1963) The kinetics of enzyme-catalyzed reactions with two or more substrates or products. I. Nomenclature and rate equations. *Biochim Biophys Acta* 67: 104–137.
- Nanba H, Takaoka Y, Hasegawa J (2003) Purification and characterization of formate dehydrogenase from *Ancyclobacter aquaticus* strain KNK607M, and cloning of the gene. *Biosci Biotechnol Biochem* 64: 720–728.
- Watanabe T, Fujiwara T, Umezawa T, Shimada M, Hattori T (2008) Cloning of a cDNA encoding a NAD-dependent formate dehydrogenase involved in oxalic acid metabolism from the white-rot fungus *Ceriporiopsis subvermispora* and its gene expression analysis. *FEMS Microbiol Lett* 279: 64–70.
- Shinoda T, Satoh T, Mineki S, Iida M, Taguchi H (2002) Cloning, nucleotide sequencing, and expression in *Escherichia coli* of the gene for formate dehydrogenase of *Paracoccus* sp. 12-A, a formate-assimilating bacterium. *Biosci Biotechnol Biochem* 66: 271–276.
- Nanba H, Takaoka Y, Hasegawa J (2003) Purification and characterization of an  $\alpha$ -halo-ketone-resistant formate dehydrogenase from *Thiobacillus* sp. strain KNK65MA, and cloning of the gene. *Biosci Biotechnol Biochem* 67: 2145–2153.
- Chenault HK, Whitesides GM (1987) Regeneration of nicotinamide cofactors for use in organic synthesis. *Appl Biochem Biotechnol* 14: 147–197.
- De Bok FAM, Hagedoorn PL, Silva PJ, Hagen WR, Schiltz E, et al. (2003) Two W-containing formate dehydrogenases (CO<sub>2</sub>-reductases) involved in syntrophic propionate oxidation by *Syntrophobacter fumaroxidans*. *Eur J Biochem* 270: 2476–2485.
- Axley MJ, Bock A, Stadtman TC (1991) Catalytic properties of an *Escherichia coli* formate dehydrogenase mutant in which sulfur replaces selenium. *Proc Natl Acad Sci U S A* 88: 8450–8454.
- Chen GT, Axley MJ, Hacia J, Inouye M (1992) Overproduction of a selenocysteine-containing polypeptide in *Escherichia coli*: The *fdhF* gene product. *Mol Microbiol* 6: 781–785.
- Gladyshev VN, Boyington JC, Khangulov SV, Grahame DA, Stadtman TC, et al. (1996) Characterization of crystalline formate dehydrogenase H from *Escherichia coli*: Stabilization, EPR spectroscopy, and preliminary crystallographic analysis. *J Biol Chem* 271: 8095–8100.
- Schuchmann K, Muller V (2013) Direct and reversible hydrogenation of CO<sub>2</sub> to formate by a bacterial carbon dioxide reductase. *Science* 342: 1382–1385.
- Scheer M, Grote A, Chang A, Schomburg I, Munnaretto C, et al. (2011) BRENDA, the enzyme information system in 2011. *Nucleic Acids Res* 39: D670–D676.
- Tishkov VI, Popov VO (2004) Catalytic mechanism and application of formate dehydrogenase. *Biochemistry (Moscow)* 69: 1252–1267.
- Ordu EB, Sessions RB, Clarke AR, Karagüler NG (2013) Effect of surface electrostatic interactions on the stability and folding of formate dehydrogenase from *Candida methylca*. *J Mol Catal B: Enzym* 95: 23–28.
- Hayashi H, Ogo S, Abura T, Fukuzumi S (2003) Accelerating effect of a proton on the reduction of CO<sub>2</sub> dissolved in water under acidic conditions. Isolation, crystal structure, and reducing ability of a water-soluble ruthenium hydride complex. *J Am Chem Soc* 125: 14266–14267.
- Huang YH, Zhang TC (2004) Effects of low pH on nitrate reduction by iron powder. *Water Res* 38: 2631–2642.
- Kumar B, Llorente M, Froehlich J, Dang T, Sathrum A, et al. (2012) Photochemical and photoelectrochemical reduction of CO<sub>2</sub>. *Annu Rev Phys Chem* 63: 541–569.
- Kim S, Kim MK, Lee SH, Yoon S, Jung KD (2014) Conversion of CO<sub>2</sub> to formate in an electroenzymatic cell using *Candida boidinii* formate dehydrogenase. *J Mol Catal B: Enzym* 102: 9–15.
- Wichmann R, Vasic-Racki D (2005) Cofactor regeneration at the lab scale. *Adv Biochem Eng Biotechnol* 92: 225–260.
- Wu JT, Wu LH, Knight JA (1986) Stability of NADPH: Effect of various factors on the kinetics of degradation. *Clin Chem* 32: 314–319.
- Lee HJ, Lee SH, Park CB, Won K (2011) Coenzyme analogs: excellent substitutes (not poor imitations) for electrochemical regeneration. *Chem Commun* 47: 12538–12540.
- Larkin MA, Blackshields G, Brown NP, Chenna R, McGettigan PA, et al. (2007) Clustal W and Clustal X version 2.0. *Bioinformatics* 23: 2947–2948.

**Author Contributions**

Conceived and designed the experiments: SHL KDJ YHK. Performed the experiments: HC JCJ DHC MHK. Analyzed the data: SHL KDJ YHK. Contributed reagents/materials/analysis tools: DHC KDJ. Wrote the paper: HC JCJ YHK.

50. Gouet P, Courcelle E, Stuart DI, Métoz F (1999) ESPript: Analysis of multiple sequence alignments in PostScript. *Bioinformatics* 15: 305–308.
51. Popov VO, Lamzin VS (1994) NAD<sup>+</sup>-dependent formate dehydrogenase. *Biochem J* 301: 625–643.
52. Schwede T, Kopp J, Guex N, Peitsch MC (2003) SWISS-MODEL: An automated protein homology-modeling server. *Nucleic Acids Res* 31: 3381–3385.
53. Nilov DK, Shabalin IG, Popov VO, Švedas VK (2011) Investigation of formate transport through the substrate channel of formate dehydrogenase by steered molecular dynamics simulations. *Biochemistry (Moscow)* 76: 172–174.